Figure 3. Patterns of immunohistochemical findings in BMD with RV. Representative transverse serial sections of biopsied skeletal muscles from BMD patients with RV. **A–C:** mGT shows the presence of RVs (**arrowheads**). **D–F:** LC3, **G–I:** Aβ1-42, **J–L:** polyUb, and **M–O:** p62. Immunofluorescent signals are seen within the fibers with RVs (**arrowheads**). Pattern 1 (left column) shows similar characteristic staining of RV fibers as DMRV and sIBM. Pattern 2 (center column) show almost similar characteristics as pattern 1, except for the faint staining of Aβ1-42. Pattern 3 (right column), with rare occurrence, shows myofibers with RVs that are negatively stained by LC3 and Aβ1-42. Scale bar: 25 μm.
doi:10.1371/journal.pone.0052002.g003

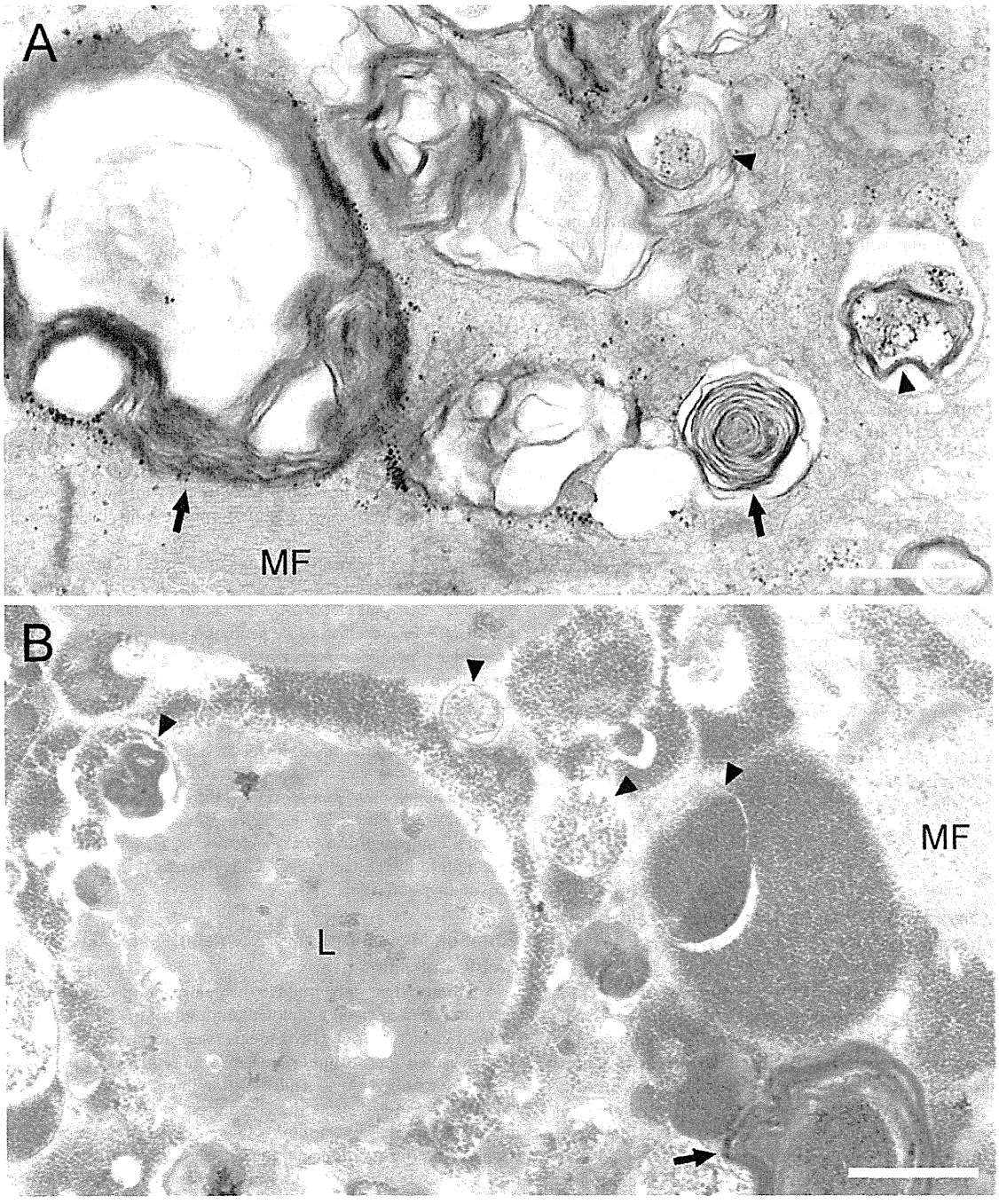

Figure 4. Areas of RVs in BMD myofibers show typical electron microscopic characteristics of autophagic vacuoles. A: Accumulation of autophagic vacuoles (**arrowheads**), various cellular debris, and multilamellar bodies (**arrow**) are seen in myofibers of some BMD patients. Note the intact arrangement of myofibrils (**MF**) surrounding autophagic area. B: In areas with or without autophagy, lipofuscin deposit (**L**) is seen. Scale bars: 1 μm.
doi:10.1371/journal.pone.0052002.g004

type 2C fibers. Positive correlation ($R^2 = 0.790$) between number of fibers with RVs and that of small atrophic fibers is seen (data not shown), suggesting a close relationship on the occurrence of RVs and the presence of atrophic myofibers.

To further characterize RVs in dystrophinopathy, we performed immunohistochemical analysis in BMD with RV patients (Figure 2, left column) in comparison with DMRV (Figure 2, center column) and sIBM (Figure 2, right column) patients; reference RVs are shown in mGT (Figure 2A–C). In RVs and areas in proximity, the lysosomal protein LAMP-1 (Figure 3D–F) and the autophagic vacuole marker LC3 (Figure 2G–I) were positively stained. As accumulation of several proteins is considered to be associated to RV formation in DMRV and sIBM [1,11,12], we observed the accumulation of APP (Figure 2J–L), Aβ1-42 (Figure 2M–O) and polyUb protein (Figure 2P–R) in and around RV in BMD with RV, DMRV and sIBM patients. We also tried to examine p62, which marks proteins for autophagic degradation in the sites with polyUb protein accumulation [13]. The staining pattern of p62 was similar to that of polyUb protein (Figure 2S–U). We also stained sections from BMD with RV, DMRV and sIBM patients with CD68 antibody, a macrophage marker, and Alexa-labeled anti-mouse IgG secondary antibody alone. Both staining were negative in RV positive fibers (Figure S1).

From our immunohistochemical analysis, we classified three patterns of staining. First, most myofibers with RV were immunoreactive to amyloid, polyUb proteins and p62 (Figure 3, left column; Pattern 1). Second, some fibers with RV showed negative for amyloid but positive for polyUb proteins and p62 (Figure 3, center column; Pattern 2). Interestingly, the third pattern consisted of some myofibers without RV that are positively stained only with polyUb proteins and p62 (Figure 3, right column; Pattern 3).

To have a closer look at the structure of these fibers with RV, we performed electron microscopy and observed the presence of autophagic vacuoles and multilamellar bodies within myofibers. In the areas surrounding autophagic vacuoles (Figure 4A), however, myofibrillar structures are almost maintained except for partial distortion of Z-line. Furthermore, lipofuscin granules were also observed around autophagic vacuoles (Figure 4B). We also confirmed Nile blue staining and confirmed that lipofuscin granules were accumulated in the fibers of BMD patients with RVs (data not shown).

Discussion

RVs in BMD are Rare but may be Related to Certain Types of *DMD* Mutations that Cause Milder Phenotype

We found 12 patients who showed RVs in muscle pathology among 65 BMD patients, representing surprising rate of 18.5%. In DMD and BMD, a genotype-phenotype correlation has been established [14–17]. Deletion of exons 45–55, for example, has been reported to be associated with quite mild muscle weakness [18–19]. Interestingly, in a previous report, one BMD patient who showed RV in his skeletal muscle section had a deletion from exons 45–48 in the *DMD* gene and showed mild to moderate weakness in lower girdle muscles [6]. In our series, the deletions in exons 45–47 or 45–48 in *DMD* gene were frequently found in the patients with RV. Our BMD with RV patients also showed a mild course of disease, with later onset and mild elevation of CK, similar as previous reports on the patients with the same deletion on *DMD* gene [6]. Additionally, in spite of similar age of disease onset in the patients with and without RV with the deletions in exons 45–47 or 45–48, the higher mean biopsy age in the patients with RV may suggest that the milder clinical course and longer disease duration in dystrophinopathy could contributory for the formation of RV in muscle. It should be noted, however, that the similar clinical course, in age of onset and biopsy, and serum CK activity, can be found in some patients in both groups, BMD with or without RV, implying that RV formation may be one of the phenotypes in patients with such deletions, or one that belongs to the disease spectrum of a mild myopathic process.

BMD Patients with RV Show Chronic Myopathic Features in Histology

Consistent with serum CK level, there were scattered necrotic and regenerating fibers observed in muscles of BMD patients without RV, while BMD patients with RV rarely show necrotic and regenerating or type 2c fibers. An increase in the number of small atrophic fibers in BMD patients with RV was remarkable as that in the patient who is previously reported [6]. This characteristic pathology is rather like myopathic changes as observed in other late-onset chronic myopathies [20].

Lipofuscin Accumulation in BMD

The number of lipofuscin granules was strikingly higher in myofibers of BMD with RV patients. Lipofuscin pigments consist of proteins and lipid containing peroxidation products of polyunsaturated fatty acids, which are formed in relation to oxidative stress, and aging process. Lipofuscin granules are highly seen in postmitotic cells and also characterized as undigested inclusion of amyloid proteins and other proteins due to lysosomal dysfunction in aged and diseased muscle and in the central nervous system [21–22].

Several papers reported that oxidative stress is implicated as a pertinent factor involved in pathogenesis of dystrophin-mutated muscular dystrophies [23,24]. In a severe DMD, dystrophin deficiency is proposed to cause profound oxidative damage, which may induce muscle necrosis that is thought to trigger the necrosis-regeneration necessary for renewal of myofibers. In contrast, in a milder BMD, although oxidative stress presumably is present at a lower level, it may lead to chronic accumulation of oxidized proteins and lipids in the absence of active necrosis and regeneration. We can only speculate that the myofibers in the BMD patients may mimic senescent status in which cellular homeostasis are slowed down. The presence of chronic myopathic changes, composed of myofiber inclusions, fiber atrophy and RV formation in BMD may reflect a long-standing process as exposed to oxidative state.

Common Mechanism of RV Formation in BMD to those in DMRV and sIBM

We found that only polyUb proteins and p62 can be seen deposited even in some fibers without and with RV. These results imply that at first, polyUb proteins were accumulated and then they recruited p62 to induce selective autophagy, as observed in neurodegenerative diseases [25]. Although in this study, we did not identify the polyUb proteins, Henderson et al. reported that the internally deleted-dystrophin minigene constructs revealed no cooperative transition during thermal denaturation and significant protein aggregation, suggesting increased susceptibility to misfolding, instability and aggregation of internally deleted-dystrophin proteins [26]. Further experiments on the identified dystrophin mutants will be required to clarify this issue.

Despite induction of autophagic process by recruitment of p62, the polyUb proteins are degraded, then leading to accumulation of numerous numbers of autophagic vacuoles. Such findings of

polyUb and p62 accumulation and numerous numbers of autophagic vacuoles and multilamellar bodies in myofibers (Figure 4A, B) are strikingly similar to those seen in a model mouse with muscle specific ablation of autophagy, implying association of accumulation of misfolded proteins and dysfunction or arrest of the autophagic process [4]. We have also found that APP, Aβ1-42, which are characteristic markers in DMRV and sIBM, as well as polyUb proteins and p62 [27–28], were accumulated in RV positive fibers. The chronic state of dysfunction or arrest of the autophagic process may secondarily cause the accumulation of amyloid proteins with long time. Interestingly, the myofibrils in the vicinity of the accumulated autophagic vacuoles maintained to be intact (Figure 4) as in those in DMRV and lysosomal myopathies [1,11]. This finding may suggest the accumulation of autophagic vacuoles is independent of contractile machinery and the accumulated proteins would not be derived from the disrupted myofibrils.

Supporting Information

Figure S1 Immunohistochemical staining of macrophage marker and secondary antibody control in RV positive fivers in BMD compared to DMRV and sIBM. Representative transverse serial sections of biopsied skeletal muscles from BMD with RV (left column), DMRV (center column) and sIBM (right column) patients. A–C: mGT staining. D–F: CD68, macrophage marker (red) co-stained with caveolin-3 (green), G–I: Alexa-labeled anti-mouse IgG secondary antibody (red) co-stained with caveolin-3 (green). Scale bar: 25 μm.
(JPG)

Acknowledgments

The authors thank the attending physicians, patients, and their families for their participation in this study. The authors also thank Ms. Kazu Iwasawa, Ms. Kaoru Tatezawa, Ms. Megumu, Ogawa, Dr. Nobuhiro Morone, and Ms. Kanako Goto (National Institute of Neuroscience, NCNP) for their technical assistance. The monoclonal antibody (H4A3) developed by J. T. August and James E.K. Hildreth was obtained from the Development Studies Hybridoma Bank (DSHB) developed under the auspices of the US National Institute of Child Health and Human Development (NICHD) and maintained by the University of Iowa, Department of Biological Sciences, Iowa City, IA 52242, USA.

Author Contributions

Conceived and designed the experiments: SN MCVM INishino. Performed the experiments: KM MCVM NM INonaka. Analyzed the data: KM SN MCVM. Contributed reagents/materials/analysis tools: YKH INonaka INishino. Wrote the paper: KM SN MCVM. Interpretation and discussion: KM SN MCVM YKH KK INishino.

References

1. Malicdan MC, Noguchi S, Nonaka I, Saftig P, Nishino I (2008) Lysosomal myopathies: an excessive build-up in autophagosomes is too much to handle. Neuromuscul Disord 18: 521–529.
2. Raben N, Takikita S, Pittis MG, Bembi B, Marie SKN, et al. (2007) Deconstructing Pompe disease by analyzing single muscle fibers: to see the world in a grain of sand. Autophagy 3: 546–552.
3. Askanas V, Engel WK (2008) Inclusion-body myositis: muscle-fiber molecular pathology and possible pathogenic significance of its similarity to Alzheimer's and Parkinson's disease brains. Acta Neuropathol 116: 583–595.
4. Malicdan MC, Noguchi S, Nishino I (2007) Autophagy in a mouse model of distal myopathy with rimmed vacuoles of hereditary inclusion body myopathy. Autophagy 3: 396–398.
5. Dalakas MC (2006) Sporadic inclusion body myositis–diagnosis, pathogenesis and therapeutic strategies. Nat Clin Pract Neurol 2: 437–447.
6. de Visser M, Bakker E, Defesche JC, Bolhius PA, van Ommen GJ (1990) An unusual variant of Becker muscular dystrophy. Ann Neurol 27: 578–581.
7. Malicdan MC, Noguchi S, Nishino I (2009) Monitoring autophagy in muscle diseases. Methods Enzymol 453: 379–396.
8. den Dunnen JT, Beggs AH (2006) Multiplex PCR for identifying *DMD* gene deletions. Curr Protoc Hum Genet Chapter 9: Unit 9.3.
9. Malicdan MC, Noguchi S, Nonaka I, Hayashi YK, Nishino I (2007) A Gne knockout mouse expressing human GNE D176V mutation develops features similar to distal myopathy with rimmed vacuoles or hereditary inclusion body myopathy. Hum Molec Genet 16: 2669–2682.
10. Takemitsu M, Nonaka I, Sugita H (1993) Dystrophin-related protein in skeletal muscles in neuromuscular disorders: immunohistochemical study. Acta Neuropathol 85: 256–259.
11. Malicdan MC, Noguchi S, Nishino I (2006) Recent advances in distal myopathy with rimmed vacuoles (DMRV) or hIBM: treatment perspectives. Curr Opin Neurol 21: 596–600.
12. Nishino I (2006) Autophagic vacuolar myopathy. Semin Pediatr Neurol 13: 90–95.
13. Kirkin V, McEwan DG, Novak I, Dikic I (2009) A role for ubiquitin in selective autophagy. Mol Cell 34: 259–269.
14. Deburgrave N, Daoud F, Llense S, Barbot JC, Récan D, et al. (2007) Protein- and mRNA-based phenotype-genotype correlations in DMD/BMD with point mutations and molecular basis for BMD with nonsense and frameshift mutations in the DMD gene. Hum Mutat 28: 183–195.
15. Koenig M, Beggs AH, Moyer M, Scherpf S, Heindrich K, et al. (1989) The molecular basis for Duchenne versus Becker muscular dystrophy: correlation of severity with type of deletion. Am J Hum Genet 45: 498–506.
16. Muntoni F, Torelli S, Ferlini A (2003) Dystrophin and mutations: one gene, several proteins, multiple phenotypes. Lancet Neurol 2: 731–740.
17. Tasaki N, Yoshida K, Haruta S, Kouno H, Ichinose H, et al. (2001) X-linked dilated cardiomyopathy with a large hot-spot deletion in the dystrophin gene. Intern Med 40: 1215–1221.
18. Ferlini A, Sewry C, Melis MA, Mateddu A, Muntoni F (1999) X-linked dilated cardiomyopathy and the dystrophin gene. Neuromuscul Disord 9: 339–346.
19. Nakamura A, Yoshida K, Fukushima K, Ueda H, Urasawa N, et al. (2008) Follow-up of three patients with a large in-frame deletion of exons 45–55 in the Duchenne muscular dystrophy (DMD) gene. J Clin Neurosci 15: 757–763.
20. Yazaki M, Yoshida K, Nakamura A, Koyama J, Nanba T, et al. (1999) Clinical characteristics of aged Becker muscular dystrophy patients with onset after 30 years. Eur Neurol 42: 145–149.
21. Seehafer SS, Pearce DA (2006) You say lipofuscin, we say ceroid: Defining autofluorescent storage material. Neurobiol Aging 27: 576–588.
22. Sugie K, Noguchi S, Kozuka Y, Arikawa-Hirasawa E, Tanaka M, et al. (2005) Autophagic vacuoles with sarcolemmal features delineate Danon disease and related myopathies. J Neuropathol Exp Neurol 64: 513–522.
23. Lawler JM (2011) Exacerbation of pathology by oxidative stress in respiratory and locomotor muscles with Duchenne muscular dystrophy. J Physiol 589: 2161–2170.
24. Vercherat C, Chung TK, Yalcin S, Gulbagci N, Gopinadhan S, et al. (2009) Stra13 regulates oxidative stress mediated skeletal muscle degeneration. Hum Mol Genet 18: 4304–4316.
25. Knaevelsrud H, Simonsen A (2010) Fighting disease by selective autophagy of aggregate-prone proteins. FEBS Lett 584: 2635–2645.
26. Henderson DM, Belanto JJ, Li B, Heun-Johnson H, Ervasti JM (2011) Internal deletion compromises the stability of dystrophin. Hum Mol Genet 20: 2955–63.
27. Broccolini A, Gidaro T, Cristofaro RD, Morosetti R, Gliubizzi C, (2008) Hyposialylation of neprilysin possibly affects its expression and enzymatic activity in hereditary inclusion-body myopathy muscle. J Neurochem105: 971–981.
28. Broccolini A, Gidaro T, Morosetti R, Mirabella M (2009) Hereditary inclusion-body myopathy: clues on pathogenesis and possible therapy. Muscle Nerve 40: 340–349.

PLOS | CURRENTS MUSCULAR DYSTROPHY

The C2A domain in dysferlin is important for association with MG53 (TRIM72)

November 5, 2012 · Advanced Diagnostics and Biomarkers

Chie Matsuda[1], Katsuya Miyake, Kimihiko Kameyama[2], Etsuko Keduka[3], Hiroshi Takeshima[4], Toru Imamura[5], Nobukazu Araki[6], Ichizo Nishino[7], Yukiko Hayashi[8]

1 Biomedical Research Institute, National Institute of Advanced Industrial Science and Technology; Department of Neuromuscular Research, National Institute of Neuroscience, National Center of Neurology and Psychiatry, **2** Biomedical Research Institute, National Institute of Advanced Industrial Science and Technology, **3** Department of Neuromuscular Research, National Institute of Neuroscience, National Center of Neurology and Psychiatry, **4** Department of Biological Chemistry, Kyoto University Graduate School of Pharmaceutical Science, **5** Biomedical Research Institute, National Institute of Advanced Industrial Science and Technology, **6** Department of Histology and Cell Biology, School of Medicine, Kagawa University, **7** Department of Neuromuscular Research, National Institute of Neuroscience, National Center of Neurology and Psychiatry; Department of Clinical Development, Translational Medical Center, National Center of Neurology and Psychiatry, **8** Department of Neuromuscular Research, National Institute of Neuroscience, National Center of Neurology and Psychiatry; Department of Clinical Development, Translational Medical Center, National Center of Neurology and Psychiatry

Matsuda C, Miyake K, Kameyama K, Keduka E, Takeshima H, Imamura T, Araki N, Nishino I, Hayashi Y. The C2A domain in dysferlin is important for association with MG53 (TRIM72). PLOS Currents Muscular Dystrophy. 2012 Nov 5 [last modified: 2012 Nov 5]. Edition 1. doi: 10.1371/5035add8caff4.

Abstract

In skeletal muscle, Mitsugumin 53 (MG53), also known as muscle-specific tripartite motif 72, reportedly interacts with dysferlin to regulate membrane repair. To better understand the interactions between dysferlin and MG53, we conducted immunoprecipitation (IP) and pull-down assays. Based on IP assays, the C2A domain in dysferlin associated with MG53. MG53 reportedly exists as a monomer, a homodimer, or an oligomer, depending on the redox state. Based on pull-down assays, wild-type dysferlin associated with MG53 dimers in a Ca2+-dependent manner, but MG53 oligomers associated with both wild-type and C2A-mutant dysferlin in a Ca2+-independent manner. In pull-down assays, a pathogenic missense mutation in the C2A domain (W52R-C2A) inhibited the association between dysferlin and MG53 dimers, but another missense mutation (V67D-C2A) altered the calcium sensitivity of the association between the C2A domain and MG53 dimers. In contrast to the multimers, the MG53 monomers did not interact with wild-type or C2A mutant dysferlin in pull-down assays. These results indicated that the C2A domain in dysferlin is important for the Ca2+-dependent association with MG53 dimers and that dysferlin may associate with MG53 dimers in response to the influx of Ca2+ that occurs during membrane injury.

To examine the biological role of the association between dysferlin and MG53, we co-expressed EGFP-dysferlin with RFP-tagged wild-type MG53 or RFP-tagged mutant MG53 (RFP-C242A-MG53) in mouse skeletal muscle, and observed molecular behavior during sarcolemmal repair; it has been reported that the C242A-MG53 mutant forms dimers, but not oligomers. In response to membrane wounding, dysferlin accumulated at the injury site within 1 second; this dysferlin accumulation was followed by the accumulation of wild-type MG53. However, accumulation of RFP-C242A MG53 at the wounded site was impaired relative to that of RFP-wild-type MG53. Co-transfection of RFP-C242A MG53 inhibited the recruitment of dysferlin to the sarcolemmal injury site. We also examined the molecular behavior of GFP-wild-type MG53 during sarcolemmal repair in dysferlin-deficient mice which show progressive muscular dystrophy, and found that GFP-MG53 accumulated at the wound similar to

wild-type mice. Our data indicate that the coordination between dysferlin and MG53 plays an important role in efficient sarcolemmal repair.

Funding Statement

This study was partly supported by intramural Research Grant 23-4 (YKH) and 23-5 (CM, IN) for Neurologicaland Psychiatric Disorders of NCNP; partly by Research on Intractable Diseases, Comprehensive Research on Disability Health and Welfare (YKH, IN), and Applying Health Technology from the Ministry of Health Labour and Welfare (IN); and partly by JSPS KAKENHI Grant Numbers of 18590966 (CM), 24390227 (YKH), and 24659437 (YKH).

Introduction

Dysferlin is a sarcolemmal protein, and dysferlin deficiency causes Miyoshi myopathy (MM) and limb girdle muscular dystrophy type 2B (LGMD2B) [1,2]. Based on the observation that dysferlin accumulates at wound sites in myofibers in a Ca^{2+}-dependent manner, dysferlin is thought to mediate Ca^{2+}-dependent sarcolemmal repair [3].

Mitsugumin 53 (MG53), also known as muscle-specific tripartite motif 72, is a recently identified protein involved in membrane repair in skeletal muscle [4]. Mice lacking MG53 suffer progressive myopathy [4], similar to dysferlin-null mice [3]. MG53 is localized in intracellular vesicles and plasma membranes in skeletal muscle, and it accumulates at injury sites in an oxidation-dependent, but not Ca^{2+}-dependent, manner [4].

MG53 interacts with dysferlin and caveolin-3 to regulate sarcolemmal repair [5]. When expressed in C2C12 myoblasts that lack endogenous MG53, damaged membrane sites cannot be repaired in the presence of GFP-dysferlin, however, co-transfection of MG53 and GFP-dysferlin in these myoblasts results in GFP-dysferlin accumulation at injury sites [5]. These findings indicated that recruitment of dysferlin to the injury site of the membrane depends on MG53. However, it remains unclear whether the absence of dysferlin perturbs recruitment of MG53 to the injury site for membrane repair. A previous report has demonstrated the association of dysferlin with MG53 with co-immunoprecipitation (IP) assays using mouse skeletal muscle and C2C12 myoblasts transfected with dysferlin and MG53 [5]. However, which protein domains participate in this interaction between dysferlin and MG53 and whether this interaction is dependent on Ca^{2+} remain unclear. MG53 oligomerizes via disulfide bonds [4] and forms homodimers via a leucine-zipper motif in the coiled-coil domain [6]. The interaction between dysferlin proteins and MG53 monomers or oligomers has not been characterized in detail. To understand the precise role of dysferlin and MG53 in sarcolemmal repair, it would be helpful to determine whether dysferlin associates with MG53 monomers, oligomers, or both in a Ca^{2+}-dependent manner.

Thus, to examine the biological role of the association between dysferlin and MG53, we used the following strategy to examine the effect of the absence of MG53 oligomers on dysferlin. We co-transfected mouse skeletal muscle with wild-type dysferlin-EGFP and RFP-tagged wild-type MG53 or a RFP-tagged MG53 mutant (RFP-C242A –MG53), and conducted a membrane-repair assay using a two-photon laser microscope. The C242A–MG53 mutant has been reported to form dimers, but not oligomers [6]. There is no report of simultaneous observation of dysferlin and MG53 during sarcolemmal repair; however, we have successfully performed real-time imaging of dysferlin-GFP and MG53-RFP after membrane injury in mouse skeletal muscle.

Dysferlin protein is absent or severely reduced in the skeletal muscle of patients with dysferlinopathy [7] and of SJL and A/J mice with mutations in the dysferlin genes [8]. To examine whether the absence of dysferlin affects the recruitment of MG53 to injury sites, we transfected skeletal muscle from dysferlin-deficient SJL and A/J mice with EGFP-MG53 and conducted membrane repair assays. These experiments are helpful in elucidating the

molecular pathology of dysferlinopathy and revealed that MG53 accumulated in the skeletal muscles of dysferlin-deficient mice, which develop progressive muscular dystrophy.

We present evidence indicating that efficient sarcolemmal repair requires both dysferlin and MG53.

Methods

Immunoprecipitation. To examine the interaction between MG53 and dysferlin, mouse gastrocnemius muscles were lysed in lysis buffer containing 20 mM Tris-HCl (pH 7.5), 150 mM NaCl, 1% NP-40, and Complete mini EDTA-free protease inhibitor cocktail (Roche) [9] supplemented with 1 mM $CaCl_2$ or 2 mM EGTA. Lysates pre-cleared with Protein A/G agarose (Pierce) were incubated with polyclonal antibodies against mouse MG53 [4] or mouse dysferlin; the anti-dysferlin antibody was made in rabbit by injecting bacterial recombinant protein containing residues 1669 to 1790. The immunoprecipitated proteins were separated by SDS-PAGE and detected on immunoblots using the same antibodies used for IP or the anti-human dysferlin monoclonal antibody, NCL-Hamlet (Novocastra Laboratories).

A human MG53 cDNA was amplified by PCR and subcloned into pFLAG-CMV-4 (Sigma). Wild-type and truncated human dysferlin that were each tagged with c-myc were generated previously [10]. We also created five truncated human dysferlin constructs with the C2A domain (aa 1-149, 1-349, and 1-1080) and without the C2A domain (aa 130-2080 and 1081-2080). The sequence of each construct was verified by DNA sequencing. FuGENE 6 or E-xtremeGENE 9 (Roche) was used to transiently transfect COS-7 cells with MG53 and wild-type or mutant dysferlin constructs. Transfectants were cultured for 48 h and subsequently lysed in the same lysis buffer used to lyse mouse muscle, except that this buffer lacked $CaCl_2$ and EGTA. Lysates pre-cleared with Protein G-Sepharose (GE Healthcare) were incubated with anti-FLAG (M2, Sigma) or anti-c-myc (9E10, Santa Cruz Biotechnology) monoclonal antibodies; Protein G-Sepharose was then added. Immunoprecipitated proteins were analyzed by immunoblotting using M2 and anti-c-myc polyclonal (A14, Santa Cruz Biotechnology) antibodies.

Pull-down assay. Fragments of the dysferlin C2A domain (corresponding to aa 1-129 of human dysferlin) were amplified as cDNA by PCR and subcloned into pGEX-5X-3 (GE Healthcare). Dysferlin p.W52R (TGG to CGG at c.527-529) and p.V67D (GTG to GAT at c.572-574) mutations were introduced by PCR using appropriate primers. GST fusion proteins expressed in BL21 *E. coli* were purified using sarkosyl [11] and bound to glutathione Sepharose 4B (GE Healthcare). COS-7 cells overexpressing FLAG-tagged human MG53 were lysed in lysis buffer containing 10 mM Na_2HPO_4, 1.8 mM KH_2HPO_4, 1% NP-40 (pH 7.4), 2 mM EGTA, various concentration of $CaCl_2$, and Complete mini EDTA-free protease inhibitor cocktail. EGTA was used to chelate the free Ca^{2+} in solution and $CaCl_2$ at various concentrations. The free calcium concentration was calculated using the free software CALCON3.6. Lysates were centrifuged to remove cellular debris, supplemented with 5 mM N-methylmaleimide (NEM) or 5 mM dithiothreitol (DTT), and finally subjected to protein cross-linking by treating with 2 mM glutaraldehyde (GA) for 5 min at room temperature, which was quenched with 100 mM Tris-HCl (pH 7.5) [6]. The cross-linked lysates were diluted with 75 mM Tris-HCl (pH 7.5), 150 mM NaCl, 1% NP-40, 2 mM EGTA, various concentrations of $CaCl_2$, and Complete mini EDTA-free protease inhibitor cocktail. Lysates pre-cleared with GST bound to glutathione Sepharose 4B were divided into aliquots and incubated with wild-type, p.W52R, and p.V67D dysferlin C2A-GST fusion protein bound to beads for 2 hr at 4°C. After three washes in lysis buffer containing 75 mM Tris-HCl (pH 7.5), 2× sample buffer (125 mM Tris-HCl (pH 6.8), 4% SDS, 20% (v/v) glycerol, and 0.004% bromophenol blue) was added to the beads, and the mixtures were incubated for 10 min at 85°C. Bound proteins were separated by SDS-PAGE and subjected to immunoblotting with the anti-FLAG antibody M2.

In vivo transfection and membrane repair assay. Twenty micrograms of N-terminal RFP-tagged human MG53 cDNA/pcDNA3.1 and/or C-terminal GFP-tagged human dysferlin cDNA/pcDNA3.1 plasmid DNA were injected into

the flexor digitorum brevis of anesthetized, 4-week-old male C57BL6J and dysferlin-deficient SJL and A/J mice. Electroporation of plasmid DNA was performed using an electric pulse generator (CUY21SC, NEPAGENE) as described previously [12]. Seven days after electroporation, skeletal muscle myocytes (for whole-mount viewing) or individual myofibers were isolated and subjected to plasma membrane injury created by a two-photon laser microscope, LSM 710NLO with GaAsp Detectors (Zeiss) and Chameleon Vision II System (Coherent)[3]. Myofiber wounding using the 820-nm infrared laser and resealing analysis based on the kinetics and extent of FM1-43 or 4-46 dye (Molecular Probes) entry through open disruptions was carried out as previously described [3,13,14].

Ethics Statement. All experiments involving animals were performed according to the Procedure for Handling Experiments involving Animals of AIST (National Institute of Advanced Industrial Science and Technology) and approved by the Institutional Animal Care and Use Committee of AIST.

Results

Association of MG53 and dysferlin in mouse skeletal muscle

We used an IP assay with protein from mouse muscle to confirm that endogenous MG53 associates with dysferlin *in vivo*. MG53 and dysferlin associated only in the absence of EGTA and $CaCl_2$ (Fig. 1). The same result was obtained using C2C12 myotubes (data not shown). MG53 was specifically co-immunoprecipitated by the anti-dysferlin antibody, and conversely dysferlin was specifically co-immunoprecipitated by the anti-MG53 antibody. Thus, we confirmed that endogenous MG53 and endogenous dysferlin form a protein complex in mouse skeletal muscle without EGTA or $CaCl_2$ supplementation.

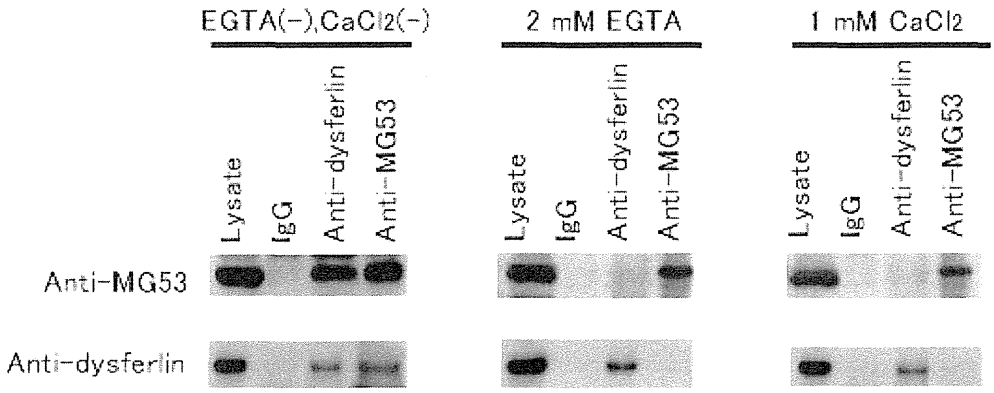

Fig. 1: IP assay of dysferlin and MG53.

MG53interacts with dysferlin in mouse skeletal muscle. Extracts from wild-type mouse skeletal muscle were subjected to IP with polyclonal anti-MG53 antibodies or polyclonal anti-dysferlin antibodies. Immunoprecipitated proteins were subjected to SDS-PAGE and visualized on immunoblots treated with the same antibodies that were used for IP.

Identification of the MG53-associating domain of dysferlin

Next, we used IP to define the region of dysferlin that associates with MG53. Specifically, we used transient co-transfection to introduce a construct encoding full-length human MG53 tagged with FLAG and a construct encoding human dysferlin tagged with c-myc into COS-7 cells; for each co-transfection, full-length dysferlin or one of five deletion mutant forms of tagged dysferlin was used (Fig. 2). For deletion mutants that lacked the C-terminal domain of dysferlin, the transmembrane domain of dysferlin was retained to increase protein stability [10]. Transfectants were lysed in the same buffer that was used for IP assays of mouse skeletal muscle extract, except that this buffer lacked EGTA and $CaCl_2$. Full-length dysferlin and deletion mutants that retained the N-terminal C2 (C2A) domain of dysferlin were co-immunoprecipitated by anti-MG53 antibody. In contrast, dysferlin mutants that lacked this N-terminal domain, Δ2-1080 and Δ2-129, failed to interact with MG53. These results indicated that the C2A domain of dysferlin was necessary for association with MG53.

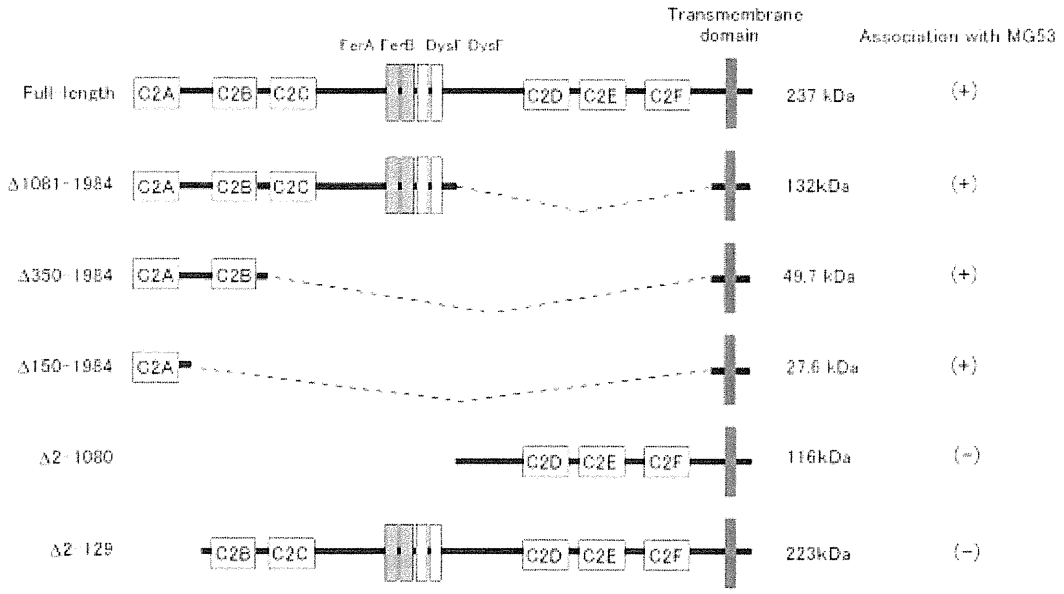

Fig. 2: Identification of MG53-binding region of dysferlin.

The dysferlin C2A domain associates with MG53. Constructs encoding dysferlin deletion mutants were used for co-IP assays, and the results of these experiments are shown on the right. Deletion mutants encoding c-myc-tagged dysferlin mutants and FLAG-tagged full-length MG53 were co-expressed in COS-7 cells. IP and immunoblotting were performed using antibodies against the c-myc and FLAG tags. MG53 was co-immunoprecipitated with full-length dysferlin and the dysferlin mutants that lacked the C-terminus, but not with the dysferlin mutants that lacked the N-terminus.

Characterization of the association of dysferlin C2A domain with MG53 monomers and MG53 oligomer

C2 domains are known to bind to phospholipids and/or proteins in a Ca^{2+}-dependent or Ca^{2+}-independent manner [15]. Therefore, we used a pull-down assay to examine whether the Ca^{2+} concentration affected the association between MG53 and the dysferlin C2A domain. We used lysis buffer containing 75 mM Tris to reduce the change in pH that can result from the addition of $CaCl_2$, to examine the calcium-dependency of the association between dysferlin and MG53. Reportedly, MG53 can exist as a monomer or an oligomer, depending on the redox state [4]. We used DTT for monomerization of MG53 by reducing sulfhydryl groups. Addition of 5 mM DTT resulted in complete dissociation of all MG53 oligomers (Fig. 3). To conduct a pull-down assay for MG53 oligomers, we treated cell lysates with an alkylating reagent, NEM, which reacts with sulfhydryl groups to form stable thioether bonds [6]. Multimers of MG53 were stabilized by chemical cross-linking with GA. Addition of 5 mM NEM to cell lysates resulted in oligomerization of MG53 (Fig. 3). In the presence or absence of Ca^{2+}, MG53 oligomers associated with wild-type C2A-GST, whereas MG53 monomers did not associate with wild-type C2A-GST. In the absence of DTT or NEM, MG53 existed as oligomers including dimers, which associated with WT C2A-GST only in 10 mM free Ca^{2+} (Fig. 3, top).

Next, we generated two mutant versions of C2A-GST (W52R or V67D) to further characterize the association between MG53 and the C2A domain. A V67D missense mutation in the human dysferlin gene has been found in patients with MM and patients with LGMD2B [16]; similarly, the W52R dysferlin missense mutation has been found in patients with LGMD2B [17]. Each mutant C2A-GST, like the wild-type C2A, associated with MG53

oligomers when conditions included NEM in the presence or absence of Ca^{2+} (Fig. 3). However, the V67D mutation altered the calcium sensitivity of the association between C2A-GST and MG53 dimers; specifically, V67D-C2A-GST could associate with MG53 when conditions did not include NEM in the absence of Ca^{2+}. In contrast, W52R-C2A-GST did not associate with MG53 when conditions did not include NEM in the presence or absence of Ca^{2+}. These results revealed that the V67D mutation in the dysferlin C2A domain altered the Ca^{2+}-dependence of the association between dysferlin and MG53 dimers.

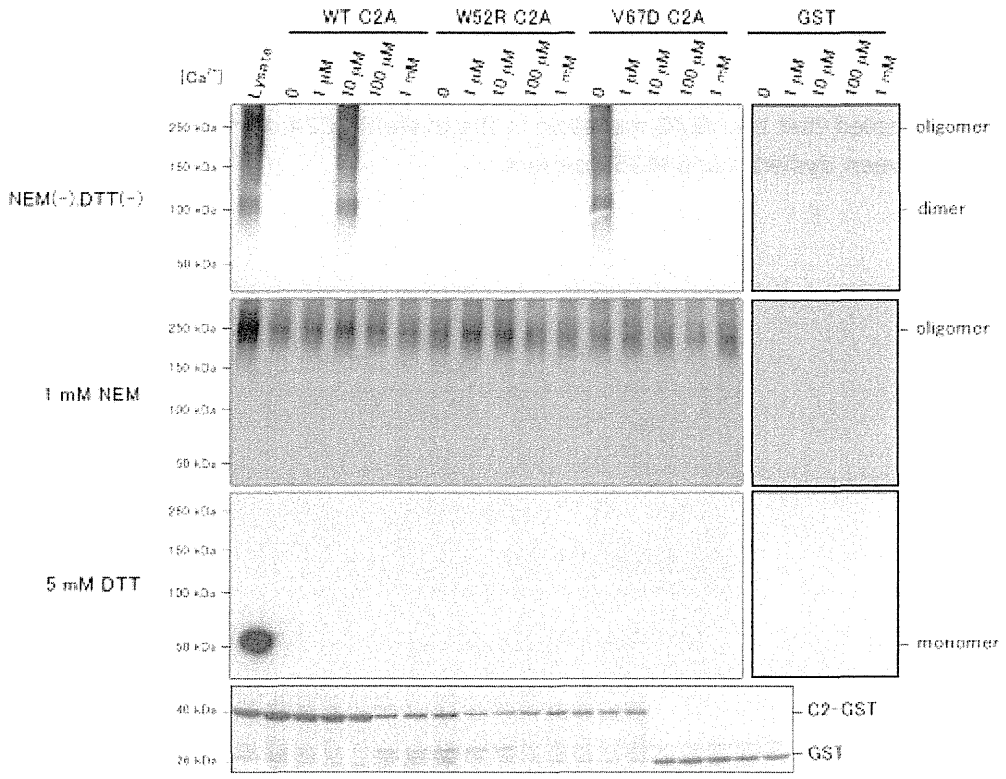

Fig. 3: Pull-down assay of dysferlin C2A-GST and MG53.

COS-7 cells overexpressing FLAG-tagged MG53 were lysed and supplemented with DTT or NEM, and proteins in these lysates were cross-linked with GA. Cross-linked proteins were incubated with glutathione Sepharose 4B beads bound to wild-type C2A-GST, V67D C2A-GST, or GST. GST fusion proteins bound to beads were separated by SDS-PAGE, followed by Coomassie Brilliant Blue R-250-staining. Precipitated MG53 oligomers/monomers were detected on immunoblots using an anti-FLAG antibody. Mutations in the C2A domain affect the association of between dysferlin and MG53.

MG53 with a C242A missense mutation shows impaired accumulation at wound sites and attenuates the formation of dysferlin patches

To examine the biological role of the association between dysferlin and MG53 in sarcolemmal repair, we used mouse skeletal muscle co-transfected with dysferlin-EGFP and RFP-tagged wild-type MG53 or RFP-tagged mutant MG53 to perform a membrane repair assay. The mutant MG53 carried a C242A missense mutation and is designated RFP-C242A-MG53 here. MG53 with a C242A missense mutation reportedly exists as a monomer or dimer when expressed in mammalian cells, but does not form oligomers via disulfide bonding [4,6]. RFP-C242A-MG53 did not accumulate at wound sites as reported previously, and it was associated with defective sarcolemmal repair [4]. Co-expression of RFP-C242A-MG53 did not affect the subcellular localization of dysferlin in myofibers, and dysferlin was localized in a striated pattern (Fig. 4A). However, RFP-C242A-MG53 compromised the accumulation of dysferlin at injury sites (Fig. 4A, B). When the movement of dysferlin and wild-type MG53 were observed simultaneously in mouse skeletal muscle, RFP-wild-type MG53 accumulated more slowly at injury sites than dysferlin-EGFP (Fig. 4A). Accumulation of dysferlin-EGFP at wound sites stops within 5 seconds of injury and disperses gradually, while wild-type MG53 continues to accumulate for 200 seconds after injury (Fig. 4A and 4B).

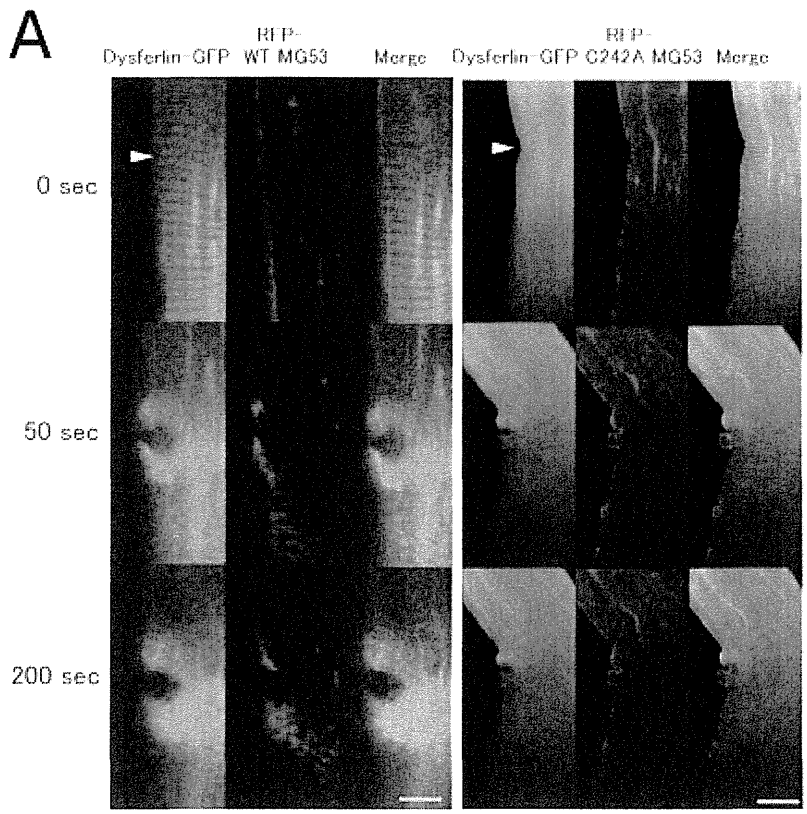
A
RFP-
Dysferlin-GFP WT MG53
Merge
RFP-
Dysferlin-GFP C242A MG53
Merge
0 sec
50 sec
200 sec

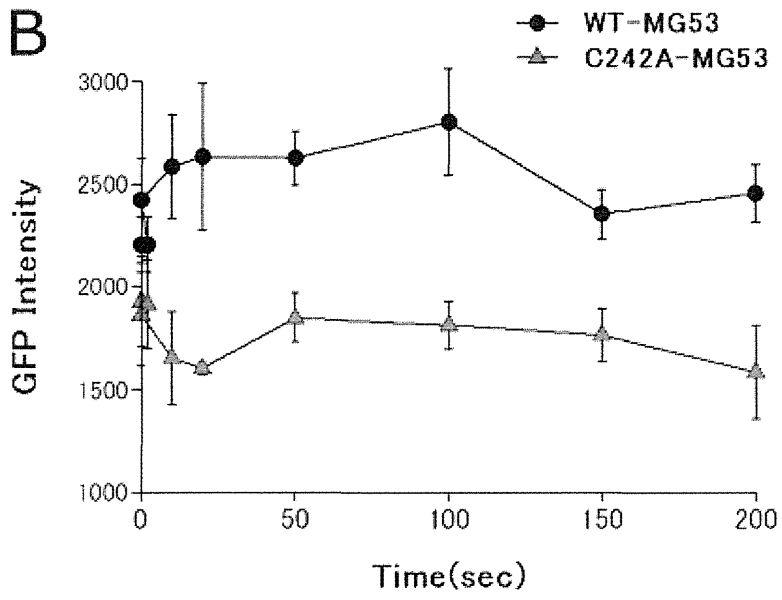

Fig. 4: Membrane repair assay of myofiber transfected with dysferlin-GFP and RFP-MG53.

RFP-C242A MG53 perturbed the accumulation of dysferlin at wound sites in the sarcolemma. A. Dysferlin-GFP was simultaneously expressed with RFP-tagged wild-type MG53 or the RFP-C242A-MG53 mutant in mouse skeletal muscle. Arrowheads indicate sites of membrane injury, which were induced with a two-photon laser microscope. Dysferlin-GFP accumulated at the injury site in the presence of RFP-wild-type MG53, but no obvious accumulation of dysferlin-GFP was observed in the presence of the RFP-C242A-MG53 mutant. Scale bar, 10 mm. B.Time course fluorescence intensity (n=3) at wounded sites versus time. For every image taken, the fluorescence intensity of dysferlin-GFP at the site of the damage (circle of 5 mm in diameter) was measured with Zeiss LSM5 Image Examinar software. Data are means ± standard deviation.

MG53 accumulates normally at injury site of sarcolemma in dysferlin-deficient mice.

A previous study revealed that exogenous expression of MG53 in undifferentiated C2C12 cells was necessary for recruitment of GFP-dysferlin to sites of injury [5]. Conversely, to examine whether the recruitment of MG53 requires dysferlin, and to elucidate the molecular pathology of dysferlinopathy, we used skeletal muscle from dysferlin-deficient A/J mice transfected with EGFP-MG53 to perform a membrane repair assay. We confirmed that EGFP-MG53 accumulated at sites of injury (Fig. 5). Sarcolemmal repair was observed and confirmed by FM4-46-loading in A/J mice (data not shown). The accumulation of MG53 at the sarcolemmal wound was observed in A/L mice, similar to wild-type mice. Similar results were obtained from the membrane repair assay using dysferlin-deficient SJL mice.

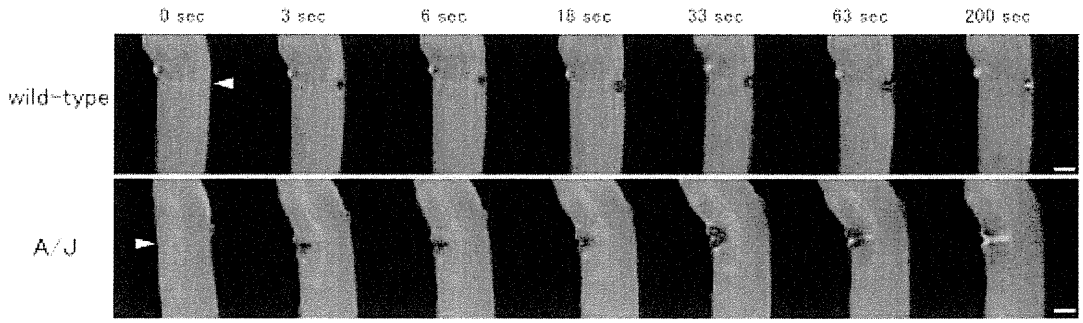

Fig. 5: Membrane repair assay of myofiber using dysferlin-deficient myofiber transfected with GFP-MG53.

GFP-MG53 accumulated at sites of injury in the sarcolemma in dysferlin-deficient A/J mice, similar to wild-type mice. GFP-MG53 was expressed in wild-type or dysferlin-deficient A/J mice, and a membrane repair assay was performed using transfected myofibers. Subcellular localization of GFP-MG53 was similar between wild-type and A/J mice. Arrowheads indicate membrane injury sites, which were induced with a two-photon laser microscope. Scale bar, 10 μm.

Discussion

Both dysferlin and MG53 are involved in membrane repair after injury in skeletal muscle. Dysferlin accumulates at wounded sarcolemmal sites, and this accumulation requires the influx of Ca^{2+} into the myofiber [3]. MG53 forms oligomers at the sarcolemmal injury site in an oxidation-dependent manner [4,6]. MG53 associates with dysferlin and facilitates vesicle trafficking to the site of membrane injury, and a recent finding suggests that MG53 and dysferlin may form a complex that participates in membrane repair in striated muscle [5]. To characterize the association between dysferlin and MG53, we used an IP assay and mouse muscle extract with or without exogenously added EGTA or $CaCl_2$ to examine the Ca^{2+} dependency of this association. Using lysis buffer that lacked EGTA and $CaCl_2$, we observed the association of dysferlin with MG53 in mouse skeletal muscle. Lysates lacking exogenously added EGTA and $CaCl_2$ contain physiological concentrations of free calcium. Hence, low concentrations of calcium are likely to be necessary for the interaction between MG53 and dysferlin.

Our results indicated that MG53 oligomers associated with the dysferlin C2A domain in the presence or absence of Ca^{2+}, whereas MG53 dimers associated with the dysferlin C2A domain in a Ca^{2+}-dependent manner. We also revealed that pathogenic mutations in the dysferlin C2A domain (W52R and V67D) alter the association between this domain and MG53 dimers in a pull-down assay. In the absence of EGTA or Ca^{2+}, dysferlin with a C2A missense mutation (W52R or V67D) did not associate with MG53 in an IP assay that used extracts from co-transfected COS-7 cells; however, full-length dysferlin with the most common pathogenic mutation found in Japan, a W999C missense mutation in the dysferlin domain, did associate with MG53 in these IP assays (data not shown). These results indicate that the dysferlin C2A domain is important for the association between dysferlin and MG53. Amino acid W52 in human dysferlin is located between the b5-sheet and the b6-sheet, and V67 is located in the b6-sheet [18]. Both residues are reportedly important for the C2 structure, particularly those of the b-sheet, and are predicted to coordinate calcium [18].

Recently, MG53 was reported to form homodimers, which are essential for MG53-mediated sarcolemmal repair [6]. We used pull-down assays to investigate associations between MG53 monomers or MG53 dimers and the

dysferlin C2A domain, and we found that MG53 dimers associated with dysferlin in a Ca^{2+}-dependent manner. An increase in the cytoplasmic Ca^{2+} level is necessary for dysferlin accumulation at wounded sarcolemmal sites [3]. The intracellular Ca^{2+} level is maintained at 50-100 nM in resting mammalian cells, but this increases to 6 μM after membrane puncture in Swiss-3T3 cells [19]. The influx of extracellular Ca^{2+} through the wound site is required for vesicle fusion with the plasma membrane and formation of a repair patch in skeletal muscle, but MG53 trafficking to the wound site does not require Ca^{2+} [4]. In pull-down assays in the present study, we demonstrated a selective association between the wild-type dysferlin C2A domain and MG53 dimers at a free Ca^{2+} concentration of 10 μM, but not at lower or higher free Ca^{2+} concentrations. These findings indicated that the concentration of free Ca^{2+} is important for association of dysferlin with MG53 dimers, and suggest that MG53 dimers not only form oligomers, but also associate with dysferlin in response to sarcolemmal injury. The altered Ca^{2+} sensitivity of the association between dysferlin with a mutation in the C2A domain and MG53 dimers in the pull-down assay also suggested that the C2A domain was important in the Ca^{2+}-dependent association between dysferlin and MG53 dimers.

We were able to analyze the movement of dysferlin and MG53 in real time during sarcolemmal repair in a membrane repair assay that employs mouse myofibers that express dysferlin-EGFP and RFP-MG53. This is the first report to demonstrate that dysferlin and MG53 have different accumulation patterns at wound sites, and this result indicated that dysferlin and MG53 have different functions in sarcolemmal repair. Our studies also revealed that MG53 carrying a C242A missense mutation can suppress the accumulation of dysferlin at the wound site; this finding, together with results from pull-down assays, suggests that MG53 dimers play an important role in sarcolemmal repair.

Our studies also revealed that MG53 accumulated at injury sites in the sarcolemma in dysferlin-deficient mice, similar to wild-type mice. However, dysferlin-deficient SJL and A/J mice have a progressive muscular dystrophy phenotype, suggesting that MG53 is necessary but not sufficient for efficient sarcolemmal repair.

Competing Interests

The authors have declared that no competing interests exist.

Correspondence

Address for correspondence : c-matsuda@aist.go.jp (C. Matsuda)

References

1. Liu J, Aoki M, Illa I, Wu C, Fardeau M, et al. (1998) Dysferlin, a novel skeletal muscle gene, is mutated in Miyoshi myopathy and limb girdle muscular dystrophy. Nat Genet 20: 31-36.

2. Bashir R, Britton S, Strachan T, Keers S, Vafiadaki E, et al. (1998) A gene related to Caenorhabditis elegans spermatogenesis factor fer-1 is mutated in limb-girdle muscular dystrophy type 2B. Nat Genet 20: 37-42.

3. Bansal D, Miyake K, Vogel SS, Groh S, Chen CC, et al. (2003) Defective membrane repair in dysferlin-deficient muscular dystrophy. Nature 423: 168-172.

4. Cai C, Masumiya H, Weisleder N, Matsuda N, Nishi M, et al. (2009) MG53 nucleates assembly of cell membrane repair machinery. Nat Cell Biol 11: 56-64.

5. Cai C, Weisleder N, Ko JK, Komazaki S, Sunada Y, et al. (2009) Membrane repair defects in muscular dystrophy are linked to altered interaction between MG53, caveolin-3 and dysferlin. J Biol Chem.

6. Hwang M, Ko JK, Weisleder N, Takeshima H, Ma J (2011) Redox-dependent oligomerization through a leucine zipper motif is essential for MG53-mediated cell membrane repair. Am J Physiol Cell Physiol 301: C106-114.

7. Tagawa K, Ogawa M, Kawabe K, Yamanaka G, Matsumura T, et al. (2003) Protein and gene analyses of dysferlinopathy in a large group of Japanese muscular dystrophy patients. J Neurol Sci 211: 23-28.

8. Ho M, Post CM, Donahue LR, Lidov HG, Bronson RT, et al. (2004) Disruption of muscle membrane and phenotype divergence in two novel mouse models of dysferlin deficiency. Hum Mol Genet 13: 1999-2010.

9. Cai C, Masumiya H, Weisleder N, Pan Z, Nishi M, et al. (2009) MG53 regulates membrane budding and exocytosis in muscle cells. J Biol Chem 284: 3314-3322.

10. Matsuda C, Kameyama K, Tagawa K, Ogawa M, Suzuki A, et al. (2005) Dysferlin interacts with affixin (beta-parvin) at the sarcolemma. J Neuropathol Exp Neurol 64: 334-340.

11. Frangioni JV, Neel BG (1993) Solubilization and purification of enzymatically active glutathione S-transferase (pGEX) fusion proteins. Anal Biochem 210: 179-187.

12. Aihara H, Miyazaki J (1998) Gene transfer into muscle by electroporation in vivo. Nat Biotechnol 16: 867-870.

13. Cho W, Stahelin RV (2006) Membrane binding and subcellular targeting of C2 domains. Biochim Biophys Acta 1761: 838-849.

14. Davis DB, Doherty KR, Delmonte AJ, McNally EM (2002) Calcium-sensitive phospholipid binding properties of normal and mutant ferlin C2 domains. J Biol Chem 277: 22883-22888.

15. Illarioshkin SN, Ivanova-Smolenskaya IA, Greenberg CR, Nylen E, Sukhorukov VS, et al. (2000) Identical dysferlin mutation in limb-girdle muscular dystrophy type 2B and distal myopathy. Neurology 55: 1931-1933.

16. De Luna N, Freixas A, Gallano P, Caselles L, Rojas-Garcia R, et al. (2007) Dysferlin expression in monocytes: a source of mRNA for mutation analysis. Neuromuscular disorders : NMD 17: 69-76.

17. Therrien C, Di Fulvio S, Pickles S, Sinnreich M (2009) Characterization of lipid binding specificities of dysferlin C2 domains reveals novel interactions with phosphoinositides. Biochemistry 48: 2377-2384.

18. Steinhardt RA, Bi G, Alderton JM (1994) Cell membrane resealing by a vesicular mechanism similar to neurotransmitter release. Science 263: 390-393.

Journal of the Neurological Sciences 318 (2012) 100–105

Contents lists available at SciVerse ScienceDirect

Journal of the Neurological Sciences

journal homepage: www.elsevier.com/locate/jns

Heterozygous UDP-GlcNAc 2-epimerase and *N*-acetylmannosamine kinase domain mutations in the *GNE* gene result in a less severe GNE myopathy phenotype compared to homozygous *N*-acetylmannosamine kinase domain mutations

Madoka Mori-Yoshimura [a,*], Kazunari Monma [b], Naoki Suzuki [c], Masashi Aoki [c], Toshihide Kumamoto [d], Keiko Tanaka [e], Hiroyuki Tomimitsu [f], Satoshi Nakano [g], Masahiro Sonoo [h], Jun Shimizu [i], Kazuma Sugie [j], Harumasa Nakamura [a,k], Yasushi Oya [a], Yukiko K. Hayashi [b], May Christine V. Malicdan [b], Satoru Noguchi [b], Miho Murata [a], Ichizo Nishino [b]

[a] *Department of Neurology, National Center Hospital, National Center of Neurology and Psychiatry, 4-1-1 Ogawahigashi, Kodaira, Tokyo 187-8551, Japan*
[b] *Department of Neuromuscular Research, National Institute of Neuroscience, National Center of Neurology and Psychiatry, 4-1-1 Ogawahigashi, Kodaira, Tokyo 187-8502, Japan*
[c] *Department of Neurology, Tohoku University School of Medicine, 1-1 Seiryo, Aoba-ku, Sendai 980-8574, Japan*
[d] *Department of Internal Medicine 3, Faculty of Medicine, Oita University, 1-1 Idaigaoka, Hasama, Yufu-shi, Oita 879-5593, Japan*
[e] *Department of Neurology, Kanazawa Medical University, 1-1 Daigaku, Uchinadamachi, Kahoku-gun, Ishikawa, 920-0214, Japan*
[f] *Department of Neurology and Neurological Science, Graduate School, Tokyo Medical and Dental University, Yushima 1-5-45, Bunkyo-ku, Tokyo 113-8519, Japan*
[g] *Department of Neurology, Osaka City General Hospital, 2-13-22, Miyakojimahonndoori, Miyakojima-ku, Osaka534-0021, Japan*
[h] *Department of Neurology, Teikyo University School of Medicine, Kaga 2-11-1, Itabashi-ku, Tokyo 173-8605, Japan*
[i] *Department of Neurology, Division of Neuroscience, Graduate School of Medicine, University of Tokyo, 7-3-1 Hongo, Bunkyo-ku, Tokyo 113-8655, Japan*
[j] *Department of Neurology, Nara Medical University School of Medicine, 840 Shijo, Kashihara, Nara 634-8521, Japan*
[k] *Clinical Trial Division, Division of Clinical Research, National Center Hospital of Neurology and Psychiatry, 4-1-1 Ogawahigashi, Kodaira, Tokyo 187-8551, Japan*

ARTICLE INFO

Article history:
Received 10 January 2012
Received in revised form 20 March 2012
Accepted 21 March 2012
Available online 14 April 2012

Keywords:
GNE myopathy
Distal myopathy with rimmed vacuoles
Hereditary inclusion body myopathy
Glucosamine (UDP-N-acetyl)-2-epimerase/*N*-acetylmannosamine kinase
(UDP-N-acetyl)-2-epimerase domain
N-acetylmannosamine kinase domain
Questionnaire
Natural history

ABSTRACT

Background: Glucosamine (UDP-N-acetyl)-2-epimerase/*N*-acetylmannosamine kinase (GNE) myopathy, also called distal myopathy with rimmed vacuoles (DMRV) or hereditary inclusion body myopathy (HIBM), is a rare, progressive autosomal recessive disorder caused by mutations in the *GNE* gene. Here, we examined the relationship between genotype and clinical phenotype in participants with GNE myopathy.
Methods: Participants with GNE myopathy were asked to complete a questionnaire regarding medical history and current symptoms.
Results: A total of 71 participants with genetically confirmed GNE myopathy (27 males and 44 females; mean age, 43.1 ± 13.0 (mean ± SD) years) completed the questionnaire. Initial symptoms (*e.g.*, foot drop and lower limb weakness) appeared at a mean age of 24.8 ± 8.3 years. Among the 71 participants, 11 (15.5%) had the ability to walk, with a median time to loss of ambulation of 17.0 ± 2.1 years after disease onset. Participants with a homozygous mutation (p.V572L) in the *N*-acetylmannosamine kinase domain (KD/KD participants) had an earlier disease onset compared to compound heterozygous participants with mutations in the uridine diphosphate-N-acetylglucosamine (UDP-GlcNAc) 2-epimerase and *N*-acetylmannosamine kinase domains (ED/KD participants; 26.3 ± 7.3 vs. 21.2 ± 11.1 years, respectively). KD/KD participants were more frequently non-ambulatory compared to ED/KD participants at the time of survey (80% vs. 50%). Data were verified using medical records available from 17 outpatient participants.
Conclusions: Homozygous KD/KD participants exhibited a more severe phenotype compared to heterozygous ED/KD participants.

1. Introduction

Glucosamine (UDP-N-acetyl)-2-epimerase/*N*-acetylmannosamine kinase (GNE) myopathy, also known as distal myopathy with rimmed vacuoles (DMRV), Nonaka myopathy (MIM: 605820) or hereditary inclusion body myopathy (HIBM; MIM: 600737), is an early adult-onset, progressive myopathy that affects the tibialis anterior muscle, but spares quadriceps femoris muscles [1,2]. The disease is caused by a mutation in the *GNE* gene, which encodes a bifunctional enzyme [uridine diphosphate-*N*-acetylglucosamine (UDP-GlcNAc) 2-epimerase (GNE) and *N*-acetylmannosamine kinase (MNK)] known to catalyze two rate-limiting reactions involved in cytosolic sialic acid synthesis [3–7]. Mutations in the *GNE* gene result in decreased enzymatic activity *in vitro* by 30–90% [7–10]. Therefore, hyposialylation is thought to

* Corresponding author. Tel.: +81 42 341 2711; fax: +81 42 346 1852.
E-mail address: yoshimur@ncnp.go.jp (M. Mori-Yoshimura).

0022-510X/$ – see front matter © 2012 Elsevier B.V. All rights reserved.
doi:10.1016/j.jns.2012.03.016

contribute to the pathogenesis of GNE myopathy. This is supported by the myopathic phenotype associated with a mouse model expressing the human D176V mutant GNE protein (GNE−/−hGNED176V-Tg) [11]. Muscle atrophy and weakness are prevented by oral treatment with sialic acid metabolites in this mouse model [12].

A phase I clinical trial using oral sialic acid therapy has recently been performed in Japan for the treatment of GNE myopathy (ClinicalTrials.gov; NCT01236898). A similar phase I study is currently underway in the United States (ClinicalTrials.gov; NCT01359319). Natural history and genotype–phenotype correlations need to be established for a successful phase II clinical trial for the treatment of GNE myopathy. However, only a small number of studies have been conducted that review the natural course of this disease. In addition, the presence of genotype–phenotype correlations is controversial in GNE myopathy, with most reports denying significant correlations [7]. In fact, substantial heterogeneity is observed among participants who have the same mutations. For example, few subjects with p.D176V and p.M712T mutations exhibited a normal or very mild phenotype, with disease onset after the age of 60 [3,13]. Furthermore, only a limited number of studies that analyze compound heterozygous patients are available. Nonetheless, such studies report a variable degree of severity [14–17].

To clarify the potential relationship between genotype and clinical phenotype (*i.e.*, age at onset, disease course, and current symptoms) of GNE myopathy, we performed a questionnaire-based survey of participants with confirmed GNE myopathy.

2. Participants and methods

2.1. Study population

We obtained approval for this study from the Medical Ethics Committee of the National Center of Neurology and Psychiatry (NCNP). Seventy-eight participants with known GNE myopathy were seen at 8 hospitals specializing in muscle disorders in Japan and 83 participants (not all genetically diagnosed) from the Participants Association for Distal Myopathies (PADM) were recruited. Participants provided written informed consent prior to completing the questionnaire.

A total of 75 participants completed and returned the questionnaire. Of the 75 participants analyzed, 4 were found to have only one heterozygous mutation. Because single heterozygous mutations have not been confirmed to cause GNE myopathy, these 4 participants were excluded from this study.

2.2. Study design

The present study is a retrospective and cross-sectional analysis, which includes 71 participants with genetically confirmed GNE myopathy. Clinical information was collected from participants using a questionnaire and genetic information was acquired from available medical records.

2.3. Questionnaire

Participants completed a self-reporting questionnaire regarding 1) developmental and past symptoms, 2) past and present ambulatory status, and 3) information about diagnosis and medical services (Supplementary material, original version in Japanese).

To determine developmental history, we collected the following information: 1) trouble before and/or during delivery, 2) body weight and height at birth, 3) age at first gait, 4) exercise performance during nursery, kindergarten, or school, and 5) age at onset and signs of first symptoms. Participants were also asked about the onset of 1) gait disturbance, 2) walking with assistance (*i.e.*, cane and/or orthotics and/or handrails), 3) wheelchair use, 4) loss of ambulation, and 5) current gait performance. With regard to medical history, participants were asked about 1) age at the time of first hospital visit, 2) whether or not they had symptoms at the time of visit, 3) age at the time of final diagnosis, 4) how many hospitals/clinics were visited before final diagnosis, and 5) whether a biopsy was performed.

2.4. Medical record examination

To verify the accuracy of the information provided by each participant, available medical records from 17 participants (23.9%) seen at outpatient clinics at NCNP were examined (9 males and 8 females).

2.5. Data handling and analysis

All variables were summarized using descriptive statistics, which included mean, standard deviation (SD), median, range, frequency, and percentage. Each variable was compared against age, sex, genotype, and domain mutation (*i.e.*, within the UDP-GlcNAc 2-epimerase domain: ED or *N*-acetylmannosamine kinase domain: KD). Student's *t* test was used to compare the means for each participant group (ED/ED, ED/KD and KD/KD participants). Data from the two participant groups were calculated using chi-square contingency table analysis. The time from disease onset to walking with assistance, time from disease onset to wheelchair use, and time from disease onset to loss of ambulation were evaluated using the Kaplan–Meier method with log-rank analysis. Questionnaire reliability was tested using intraclass correlation coefficients (ICCs), and two-sided 95% confidence intervals (CIs) were calculated using a one-way random effects analysis of variance model for inter-rater reliability. All analyses were performed using SPSS for Macintosh (version 18, SPSS Inc., Chicago, IL).

3. Results

3.1. General characteristics

A total of 71 Japanese individuals (27 males and 44 females) participated in the study. The mean age at data collection was 43.1 ± 10.7 years. None of the participants showed developmental abnormalities during infancy or early childhood.

3.2. GNE mutations

Forty-one percent of study participants (n = 29/71) had homozygous mutations, while 59% (n = 42/71) had compound heterozygous mutations (Table 1). Among homozygous participants, 86.2% (n = 25/29) harbored the p.V572L mutation, while the remaining participants had other mutations. No homozygous participants for the p.D176V mutation were identified. Among compound heterozygous participants, 28.5% (n = 12/42) had p.D176V/p.V572L mutations, while the remaining participants had other mutations. With respect to allelic frequency, 50.0% (71/142) were p.V572L, 20.4% (29/142) p.D176V, 3.5% (5/142) p.C13S, 2.8% (4/142) p.M712T, and 2.1% (3/142) p.A630T. All other mutations accounted for 2%. A total of 18.3% (n = 13/71) of participants were homozygous with a mutation in the GNE domain (ED/ED), 39.4% (n = 28/71) of participants were compound heterozygous with a mutation in the GNE domain and one in the MNK domain (ED/KD), and 42.3% (n = 30/71) of participants had a mutation in the MNK domain in both alleles (KD/KD).

3.3. Past and present symptoms

Mean participant age at symptom onset was 25.2 ± 9.2 years (range, 12–58 years; median, 24.5 years). There was no significant difference between males and females for current age, age at disease

Table 1
Genotypes of the GNE myopathy patient population.

		Questionnaire	Outpatients
ED/ED	Total	13	4
	Homozygote	1	0
	p.C13S homozygote	1	
	Compound heterozygote	12	4
	p.C13S/p.M29T	1	1
	p.C13S/p.A63I	1	1
	p.D176V/p.F233S	1	1
	p.D176V/p.R306Q	2	
	p.R129Q/p.D176V	1	
	p.R129Q/p.R277C	1	
	p.D27L/p.D176V	1	1
	p.B89S/p.D176V	1	
	p.D176V/p.R246W	1	
	p.D176V/p.R321C	1	
	p.D176V/p.V331A	1	
ED/KD	Total	28	8
	Compound heterozygote	28	8
	p.D176V/p.V572L	12	3
	p.C13S/p.V572L	1	1
	p.D176V/p.I472T	1	1
	p.D176V/p.L603F	1	1
	p.R177C/p.V572L	1	1
	383insT/p.V572L	1	1
	p.D176V/p.G708S	2	
	p.D187G/p.V572L	2	
	p.R8X/p.V572L	1	
	p.D176V/p.G568S	1	
	p.D176V/p.H626R	1	
	p.D176V/p.A630T	1	
	p.I276T/p.V572L	1	
	p.G295D/p.A631V	1	
	p.A600E/p.D176V	1	
KD/KD	Total	30	5
	Homozygote	28	5
	p.V572L homozygote	25	4
	p.M712T homozygote	2	
	p.A630T homozygote	1	
	Compound heterozygote	2	0
	p.V572L/p.R420X	1	1
	1756Gdel (stop)/p.V572L	1	

onset, age at walking with assistance, age at wheelchair use, and current ambulatory status. Initial symptoms included gait disturbance (66.2%, n = 47/71), other lower limb symptoms (26.8%, n = 19/71), easily fatigued (23.9%, n = 17/71), and weakness of hands and fingers (8.5%, n = 6/71). In addition, 21.1% (n = 15/71) had onset of symptoms before the age of 20. When specifically asked, 47.8% (n = 34/71) described themselves as slow runners during childhood, and 42.5% reported having had difficulty with physical exercise during school years.

3.4. Diagnosis

Mean participant age at diagnosis was 33.9 ± 12.6 years (median, 29.5 years; range 17 to 67 years). Mean participant age at first physician visit was 29.6 ± 10.4 years (median, 27 years; range, 12–62 years), and mean time between first visit and diagnosis was 4.4 ± 8.3 years.

3.5. Walking with assistance and wheelchair use

At the time of the survey, 52.0% (n = 37/71) were ambulant (41.3 ± 12.8 years); however, only 15.5% (n = 11/71, 40.0 ± 13.6 years) could walk without assistance, with the remaining 35.2% requiring assistance (n = 25/71, 41.8 ± 12.7 years). Only 7.0% of these participants (n = 5/71) could walk up stairs, while 49.3% (n = 35/71) were non-ambulant. Wheelchairs were used by 63.6% (23.9% partially bound and 43.7% totally bound) and an electric wheelchair was used by 41.9% (n = 31/71). Mean participant age of wheelchair users was 34.9 ± 11.7 years (range, 18–70 years). Wheelchairs were not used by 32.4% (n = 26/71) of participants. Current age of wheelchair-free participants was 39.4 ± 12.3 years (range, 21–61 years; median, 34 years) and that of wheelchair-bound participants was 42.8 ± 12.6 years (range, 21–71; median, 42 years).

Kaplan–Meier analysis revealed a median proportional age at walking with assistance of 30.0 ± 1.4 years. Median proportional age of wheelchair users was 36.0 ± 2.7 years, and that for loss of ambulation was 45.0 ± 4.2 years. The time from disease onset to walking with assistance was 7.0 ± 0.4 years, time from disease onset to wheelchair use was 11.5 ± 1.2 years, and time from disease onset to loss of ambulation was 17.0 ± 2.1 years.

3.6. Correlation between disease genotype and phenotype

To determine if a correlation between genotype and phenotype existed, we compared domain mutations (ED/KD, or both) available from medical reports to questionnaire answers (Table 2). Participants with KD/KD mutations (both homozygous and heterozygous) were younger and more severely affected compared to participants with ED/KD or ED/ED mutations. No significant difference in current age or age at disease onset between ED/ED and ED/KD participants was identified. Kaplan–Meier analyses revealed that the proportional time from disease onset to wheelchair use and from disease onset to loss of ambulation was significantly shorter in KD/KD compared to ED/KD participants. ED/ED participants exhibited a shorter time of disease onset to wheelchair use compared to ED/KD participants (Table 3, Fig. 1).

3.7. Comparison between p.V572L homozygous and p.D176V/p.V572L compound heterozygous participants

To compare clinical features in patients with the same mutations, we specifically analyzed data from those with p.V572L (n = 25/71, 35.2%) and p.D176V/p.V572L (n = 12/71, 16.9%) mutations, as these two were the most frequent mutations in our study population (Table 2). Age at disease onset of homozygous participants (p.V572L) was 21.3 ± 5.7 years (range, 12–32 years) and time from disease onset to wheelchair use was 11.3 ± 5.4 years (range, 3–21 years). Only 16.0% (n = 4/25) of these homozygous participants reported that they were not currently using a wheelchair. In contrast, the mean age at disease onset of heterozygous participants (p.D176V/p.V572L) was 35.5 ± 14.1 years (range, 13.5–57 years) and time from disease onset to wheelchair use was 17.9 ± 7.0 years (range, 11–28 years). A total of 66.7% of these compound heterozygous participants (n = 8/12) reported that they were not using a wheelchair.

3.8. Questionnaire response compared to medical records

Questionnaires from 17 participants (NCNP outpatient participants) were compared to available medical records (Table 2). Age at disease onset, age at onset of gait disturbance, age at walking with assistance, and age at loss of ambulation were assessed for inter-rater reliability. Age at disease onset, age at onset of gait disturbance, age at walking with assistance, and age at loss of ambulation were assessed for inter-rater reliability. ICC values were 0.979 (95% CI 0.941–0.992) for age at disease onset, 0.917 (95% CI 0.752–0.972) for age at onset of gait disturbances, 0.985 (95% CI 0.949–0.995) for age at walking with assistance, and 0.967 (95% CI 0.855–0.993) for age at loss of ambulation.

4. Discussion

The present study provides a detailed overview of disease severity and progression in 71 Japanese participants with genetically confirmed GNE myopathy. Questionnaire-based surveys have been used to study